Phase diagram of the Cu-Pd surface alloy: A first-principles calculation

R. Tétot
Laboratoire des Composés Non-Stoechiométriques, Bâtiment 415, Université de Paris–Sud, Centre d'Orsay, 91405 Orsay Cedex, France

J. Kudrnovský
Institute of Physics, Academy of Sciences of the Czech Republic, CZ-180 40 Praha 8, Czech Republic and Institute for Technical Electrochemistry, Technical University, A-1060 Vienna, Austria

A. Pasturel
Experimentation Numérique, Maison des Magistères, Centre National de la Recherche Scientifique, Boîte Postale 166, 38042 Grenoble Cedex, France and Laboratoire de Thermodynamique et Physico-Chemie Métallurgiques, Ecole Nationale d'Electrochimie et d'Electrométallurgie de Grenoble, Boîte Postale 75, 38402 Grenoble Cedex, France

V. Drchal
Institute of Physics, Academy of Sciences of the Czech Republic, CZ-180 40 Praha 8, Czech Republic

P. Weinberger
Institute for Technical Electrochemistry, Technical University, A-1060 Vienna, Austria
(Received 27 December 1994; revised manuscript received 27 February 1995)

A method that combines electronic-structure calculations with Monte Carlo simulations is applied to determine the phase diagram of the CuPd surface alloy on a Cu(001) substrate. The calculations are based on an effective Ising model with parameters as defined within the generalized perturbation method and as calculated by means of the linear-muffin-tin-orbital method. The formation of the ordered $c(2\times2)$ phase of the CuPd surface alloy on the Cu(001) substrate is discussed. The order/disorder temperature of the $c(2\times2)$ phase as well as the phase diagram is calculated using pair interactions corresponding to the 50:50 composition as well as concentration-dependent pair interactions.

I. INTRODUCTION

In recent years progress has been made in calculating alloy phase diagrams and associated thermodynamic quantities from first principles. For bulk solids, ordering and clustering phenomena are currently studied within a microscopic theory based on a generalized three-dimensional (3D) Ising model,[1] whereby the parameters can be derived from *ab initio* band-structure techniques using either the so-called Connolly-Williams inversion[2] or the generalized perturbation method (GPM).[3] First-principles phase diagrams have been presented for a variety of systems including metallic systems,[4–9] semiconductors,[5,10] and superconducting oxides,[11–13] and show that it is possible to go from electronic-structure calculations to phase diagram through a set of well-controlled approximations. This at least seems to be the case when ordering effects can be assumed to occur with respect to a fixed, rigid lattice. In principle, there is no difficulty in extending such calculations to include elastic and relaxation effects, even though this has not been yet worked out in detail. In contrast to these developments, the determination of thermodynamic properties near surfaces or other extended defects has not yet gained the same level of sophistication, despite the fact that a large number of technologically important phenomena such as catalysis, corrosion, deposition, and growth, for example, occur at or near the surface. The existence of a free surface permits both new, strain-relieving relaxations and electronically driven reconstructions, and leads to the possibility that the lowest-energy atomic topology at the free surface of an alloy is qualitatively different from that of the corresponding three-dimensional bulk. For instance, the growth of metals on metal surfaces very often gives rise to surface structures without bulk counterparts. Moreover, these surface structures persist only over a few monolayers. A complete study of the growth of metallic layers on a metallic substrate, however, is beyond the scope of the present study. In here, we assume a bulk exposed plane and study its equilibrium structure and energy. It should be noted that only recently were attempts made to generalize the GPM theory to the case of alloy surfaces. In the very first studies, an empirical tight-binding model was applied,[14] which used the recursion method and described the semi-infinite solids by a finite cluster.[15] Recently, a method[16] for the calculation of the parameters for the Ising model for semi-infinite disordered alloys within the GPM approach, based on the tight-binding linear-muffin-tin-orbital (TB-LMTO) method,[17] was developed. The first applications dealt with two important fields in surface studies, namely, (i) the explanation of the origin of formation of ordered sur-

face alloys on clean transition-metal surfaces[18] and (ii) the study of the surface composition for disordered metallic alloys and the determination of the composition profile.[19]

In the present paper we wish to address a different problem, namely, to estimate a phase diagram of a 2D alloy system, which consists of a random monolayer on a perfect nonrandom substrate. Aside from the technological importance of such system, the theoretical attraction is definitely the fact that such a system is truly 2D from a statistical point of view, i.e., randomness is limited to the overlayer, while its electronic structure corresponds to an infinite stack of substrate layers with a random monolayer on top. The Ising model parameters for the homogeneous 2D system result therefore from a strongly inhomogeneous 3D electronic structure. As compared to 3D phase diagrams, the lower dimensionality of the statistical part reduces a variety of possible superstructures and to some extent simplifies also the construction of the corresponding phase diagram. As a first application, the phase diagram of CuPd surface alloys on the Cu(001) substrate is investigated. Since such alloys are almost planar,[20] one safely can ignore any effects due to displacements from ideal lattice positions, keeping in mind, however, that a complete theory of the thermodynamic stability of such monolayers has to include these kinds of effects.

The present approach consists of three steps: (i) determination of the self-consistent electronic structure of a semi-infinite substrate with a disordered overlayer, (ii) a study of the instability of the disordered phase with respect to a formation of ordered superstructures, and (iii) a study of the thermal properties of this system by means of Monte Carlo simulations. The paper is organized as follows. In Sec. II, the key features of the Ising model for a random overlayer on perfect substrate are summarized. Section III consists of a presentation of the applied Monte Carlo simulation technique and a discussion of the results obtained for the CuPd surface phase diagram in comparison with available experimental information.

II. FORMALISM

The present approach is based on the local-density approximation (LDA) and uses the TB-LMTO method within the atomic sphere approximation for the potentials in order to determine the electronic structure of a disordered overlayer on the perfect substrate. (For details, see Refs. 21 and 22.) For the charge densities, however, monopole and dipole terms are included in the mulitpole expansion.[22] Alloy disorder is described via the coherent potential approximation (CPA) as generalized to inhomogeneous systems with only two-dimensional translational symmetry. The semi-infinite alloy is considered to be partitioned into three regions: (i) a perfect substrate with no disorder, (ii) a homogeneous vacuum region represented by empty spheres and characterized by flat potentials, and (iii) an intermediate region consisting of several (M) layers, where all inhomogeneities (chemical or electronic) are located. This region consists of a few substrate layers, the random overlayer, and a few layers of empty spheres. Only the potentials in the intermediate region are determined self-consistently, while those for the substrate or the vacuum are obtained separately for the respective infinite systems.

The Green's function $g(z)=[P(z)-S]^{-1}$ is defined in terms of the potential function matrix $P(z)$ and the structure constants matrix S. The potential functions are random but site-diagonal quantities, whereas the structure constants S, which describe the intralayers and interlayers coupling, are nonrandom site–off-diagonal quantities and short ranged.[23]

Subsequently the site–off-diagonal elements of the configurationally averaged Green's function within the overlay are needed to determine the parameters of the Ising model

$$H^I=E_0+\tfrac{1}{2}\sum_{\mathbf{R},\mathbf{R}'}\sum_{\alpha,\alpha'}V^{\alpha,\alpha'}_{\mathbf{R},\mathbf{R}'}\eta^{\alpha}_{\mathbf{R}}\eta^{\alpha'}_{\mathbf{R}'}+\cdots \quad (\alpha,\alpha'=A,B)\ . \tag{1}$$

Here E_0 is the configurationally independent part of the alloy internal energy and the $V^{\alpha,\alpha'}_{\mathbf{R},\mathbf{R}'}$ are the interatomic pair interactions. A particular configuration of the alloy is characterized by a set of occupation indices $\eta^{\alpha}_{\mathbf{R}}$, where $\eta^{\alpha}_{\mathbf{R}}=1$ if site $\mathbf{R}$ is occupied by an atom of type α, and $\eta^{\alpha}_{\mathbf{R}}=0$ otherwise. The parameters of the Ising model are found within the GPM by mapping at $T=0$ the grand-canonical potential $\Omega_{\rm el}(T=0,E_F)$ of the electronic subsystem (where E_F is the Fermi energy) onto the Hamiltonian in Eq. (1). The usual GPM expansion yields for the so-called renormalized pair interatomic interactions of Ising Hamiltonian the following expression:[16]

$$V^{\alpha\alpha'}_{\mathbf{R}\mathbf{R}'}=\frac{1}{\pi}\mathrm{Im\,tr}\int_{-\infty}^{E_F}\{\lim_{\delta\to 0^+}\ln[1-t^{\alpha}_{\mathbf{R}}(z)\bar{g}_{\mathbf{R}\mathbf{R}'}(z)\times t^{\alpha'}_{\mathbf{R}'}(z)\bar{g}_{\mathbf{R}'\mathbf{R}}(z)]\}dE\ , \tag{2}$$

where tr means the trace over the angular-momentum space and $z=E+i\delta$. The quantity $\bar{g}_{\mathbf{R}\mathbf{R}'}(z)$ is the configurationally averaged Green's function and $\mathbf{R}$ and $\mathbf{R}'$ sites in the overlayer. For a particular site $\mathbf{R}$, $t^{\alpha}_{\mathbf{R}}(z)$ is the on-site element of the single-site t matrix that corresponds to species α in the effective medium as characterized by the coherent-potential-function matrix $\mathcal{P}(z)$, which is a site-diagonal quantity with elements $\mathcal{P}_{\mathbf{R}}(z)$. The coherent potential function

$$\mathcal{P}_{\mathbf{R}}(z)=\begin{cases}\mathcal{P}_p(z)\ , & p=1,2,\ldots,M \text{ in the intermediate region}\\ P^b(z) \text{ or } P^v(z) & \text{otherwise}\ ,\end{cases} \tag{3}$$

has in general different values for the layers in the intermediate region. In (3) indices b and v refer to the substrate and the vacuum regions, respectively. In the intermediate region ($1 \leq p \leq M$), the coherent potential functions $\mathcal{P}_p(z)$ are found from a set of CPA and LDA equations.[21,22] In the present study randomness is limited to the overlayer. It should be noted that the so-called unrenormalized pair interactions corresponds to the first-order expansion of the logarithm in Eq. (2). In a similar way, triplet and higher multisite interactions can be defined.[16]

Using the transformation to the lattice-gas model, $\eta_{\mathbf{R}}^{A}=1-\eta_{\mathbf{R}}^{B}\equiv\eta_{\mathbf{R}}$, and limiting the expansion to pair interactions, the Ising Hamiltonian less a constant [see Eq. (1)] can be written as

$$H^{I}=\tfrac{1}{2}\sum_{\mathbf{R},\mathbf{R}'} \mathcal{V}_{\mathbf{R},\mathbf{R}'}\eta_{\mathbf{R}}\eta_{\mathbf{R}'} , \tag{4}$$

where

$$\mathcal{V}_{\mathbf{R}\mathbf{R}'}=V_{\mathbf{R}\mathbf{R}'}^{AA}+V_{\mathbf{R}\mathbf{R}'}^{BB}-V_{\mathbf{R}\mathbf{R}'}^{AB}-V_{\mathbf{R}\mathbf{R}'}^{BA} . \tag{5}$$

The quantities $\mathcal{V}_{\mathbf{R}\mathbf{R}'}$ are the so-called effective pair interactions as given in terms of the unrenormalized or renormalized pair interactions defined above.

It should be noted that Eq. (1) is a special case of the Ising Hamiltonian discussed in previous papers,[16,19] since randomness is limited to a single overlayer with crystallographically equivalent sites (see also Refs. 18 and 24). It is important to note that, in general, an Ising Hamiltonian for a semi-infinite random alloy represents an inhomogeneous case, in which the on-site terms are of crucial importance, for example, for surface segregation phenomena.[19] The present (homogeneous) case represents the 2D analog of the common 3D Ising Hamiltonian.

The limitations of the present approach and possible future improvements can be summarized as follows. (i) For the electronic part of the problem, the inclusion of relativistic corrections[25] may turn out to be necessary for systems containing heavy elements, in particular, for example, for the related case of the CuAu/Cu(001) system. (ii) Layer relaxations can be rather important for certain classes of system and should be included. (iii) Presently only the band part of the total energy is mapped onto the Ising model, i.e., the double-counting term is neglected. Irrespective of the dimensionality, this seems to be the main restriction of the present use of the Ising model. (iv) The GPM is usually based on electronic-structure calculations performed at $T=0$ K. Since electronic-structure calculations at finite temperatures are possible, an inclusion of electronic entropy contributions seems to be feasible. (v) The presence of magnetic moments can significantly influence order-disorder transitions and consequently the corresponding phase diagram.[3] First *ab initio* studies of this phenomenon appeared just recently.[26,24] (vi) Finally, the vibrational part of the entropy could be added to the Ising model[3] if necessary.

III. MONTE CARLO CALCULATIONS

A. Computational aspects

Once the effective Ising model has been defined, thermodynamic theories such as a mean-field Bragg-Williams approximation, the cluster variation method,[27] or the Monte Carlo simulation technique[28] can be applied to study finite-temperature properties.[1] Quite clearly the order-disorder effects for the present system can be restricted to a square lattice. For a model Ising Hamiltonian consisting of nearest-neighbor and second-nearest-neighbor pair interactions, the ground-state ordered structures are displayed in Fig. 1, namely, (a) the disordered phase, (b) an antiferromagnetic phase referred to as $c(2\times2)$ or $(\sqrt{2}\times\sqrt{2})$ structure (the latter notation refers to the lengths of the primitive vectors of the superstructure), (c) an antiferromagnetic phase referred to as (2×1) structure, and (d) a phase, referred to as (2×2) structure. While the first three ground-state structures are basically unique, for the fourth case, an infinite number of other structures can be obtained by introducing parallel conservative antiphase boundaries in the (2×2) structure. (For details, see Ref. 1.) The advantage of the square-lattice model and the model Ising Hamiltonian is that they give ground-state structures that have been observed experimentally. Typical examples are systems such as Au on Cu(001) (Refs. 29 and 30) or Pd on Cu(001).[20,31–34] In such a representation, the occurrence of the ground states depends on the sign of nearest-neighbor and second-nearest-neighbor pair interactions. In the present notation, for instance, if $\mathcal{V}_1$ is positive and $\mathcal{V}_2$ is equal to zero, the only stable ordered structure at finite temperature should be the $c(2\times2)$ structure. In the case of nonvanishing second-nearest-neighbor interactions, two different regimes occur. If $\mathcal{V}_2$ is negative, the only stable structure is the $c(2\times2)$ structure, the transition is of first

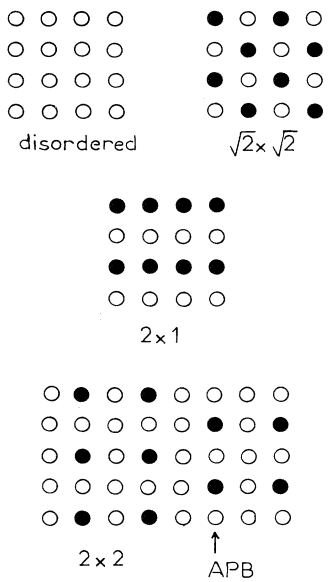

FIG. 1. Ground states for the square lattice with nearest- and second-nearest-neighbor interactions.

order at low temperatures, and there is a tricritical point.[1] If V_2 is positive, the system is frustrated and the phase diagram is expected to be more complicated (see Fig. 2). It is therefore interesting to learn whether a first-principles Ising Hamiltonian leads to a similar situation or due to the occurrence of nonvanishing pair interactions beyond the second neighbors to a more complicated one.

At low dimensionality, the mean-field theory is known to be not reliable enough. On the other hand, the Monte Carlo (MC) is one of the most powerful numerical techniques for obtaining quasiexact results from calculations made for finite systems. In order to obtain the phase digram, MC simulations have been performed in the grand canonical ensemble, using a lattice of $2\times l^2$ sites with l varying from 50 to 100, and two-dimensional periodic boundary conditions. For each temperature, the properties of the equilibrium state, as defined by the long-range-order parameter, is obtained by performing 5000–7000 MC steps/site. All these parameters allow the MC simulations to overcome the problems related to the finite size of the sample and the ones related to the determination of the equilibrium states.

B. Discussion

The formation of surface alloys on low-index transition-metal surfaces is now well established. When a Cu(001) substrate is exposed to Pd or Au at room temperature, a $c(2\times2)$ low-energy electron-diffraction (LEED) pattern is observed, which reaches its maximum intensity for a deposition of $\frac{1}{2}$ ML of Pd (Au) atoms.[20,30] The alloy character of the Cu(001)$c(2\times2)$-Pd phase has also been confirmed by photoemission experiments.[20] The Pd-coverage associated with the maximum $c(2\times2)$ LEED intensity was confirmed to be $\frac{1}{2}$ ML (Ref. 34) using Rutherford backscattering spectrometry, which provides reliable information on the coverage of a surface by foreign atoms. A $c(2\times2)$ phase was observed also for Pd coverages of more than 1/2 ML, which corresponds to the ideal ordered structure. In a previous attempt,[18] the stability of a random overlayer of CuPd on a Cu(001) substrate was studied, using a concentration fluctuation theory of ordering in alloys. The most important result was that the $Cu_{50}Pd_{50}$ alloy surface on Cu(001) is found to be more stable than the disordered $Pd_{50}Vac_{50}$ on the same substrate, where Vac denotes vacancy sites. In other words, the Pd atoms form a mixed alloy layer like a (001) face of an ordered Cu_3Au structure rather than an overlayer of atoms located at the fourfold symmetrical hollows on Cu(001).

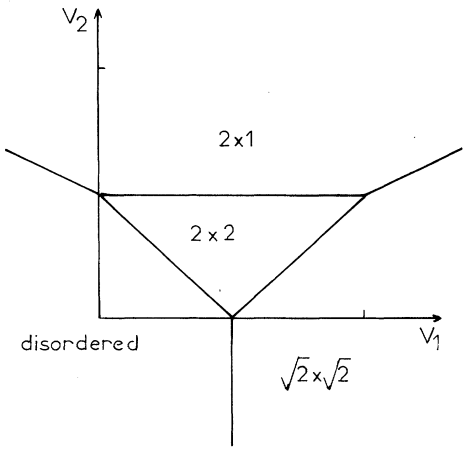

FIG. 2. Phase diagram at $T=0$ K for the square lattice with nearest- and second-nearest-neighbor interactions.

As the $c(2\times2)$ superstructure occurs at the 50:50 composition, it is tempting to model the surface phase diagram from only effective pair interactions calculated at this composition. It should be noted that such a scheme has been used in Ref. 35 to study surface-induced ordering effects. However, we will show that the composition dependence of the effective pair interactions cannot be neglected for the present system, and that the implications of this dependence are indeed considerable in particular when studying phase diagrams (basically because of the common tangent rule[1]). At the equiatomic composition, the pairwise interchange energies are 6.51, −0.59, −0.36, −0.18, −0.13, and −0.01 mRy for the first six neighbor shells in the $Cu_{50}Pd_{50}$ overlayer. The remaining pair and all triplet interactions are of the order of 0.1 mRy or less. Clearly, the nearest-neighbor interaction dominates. The dominating positive nearest-neighbor-interchange interaction implies a robust ordering tendency for the CuPd surface alloy. Small but negative second- and third-nearest-neighbor pair interactions further enhance the tendency to form a $c(2\times2)$ phase. It should be noted that the pairwise interactions between the third-nearest neighbors are only two times smaller than the ones between the second-nearest neighbors; therefore, they cannot be neglected. Consequently, in order to obtain a quantitative description of the phase diagram of the CuPd surface alloy on the Cu(001) substrate, the MC simulations are performed using the five first-nearest-neighbor pair interactions. The corresponding phase diagram using the pairwise interchange energies as calculated for the 50:50 concentration is displayed in Fig. 3. It shows a strong stability of the $c(2\times2)$ phase and is symmetric with respect to the 50:50 concentration due to the missing composition dependence of the effective pair interactions. At this concentration, the critical temperature of the second-order transition is around 660 K. The stability range of the $c(2\times2)$ is relatively large at room temperature, namely from 35% Cu to 65% Cu. The transition becomes first-order at about 110 K, with the occurrence of two domains. On the Cu-rich side, the domain is formed by a mixture of pure Cu and a $c(2\times2)$ phase while oppositely, the second domain represents a mixture of pure Pd and a $c(2\times2)$ phase.

Taking the composition dependence of the effective pair interactions into account, the pairwise interaction energies for the first six shells in $Cu_{25}Pd_{75}$ are 5.59, −1.10, −0.22, −0.20, −0.02, and 0.22 mRy, while in $Cu_{75}Pd_{25}$ they are 7.70, 0.04, −0.07, 0.12, 0.0, and −0.06 mRy. All other pair and all triplet interactions are less than 0.15 mRy. There is a dominating tendency towards ordering also in these nonstoichiometric cases, connect-

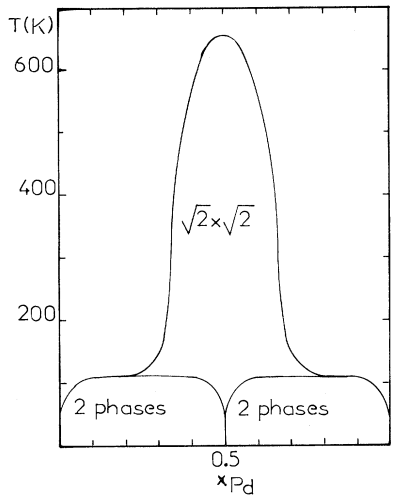

FIG. 3. Phase diagram of the CuPd surface alloy on a Cu (001) substrate as calculated with nonconcentration-dependent pairwise interactions.

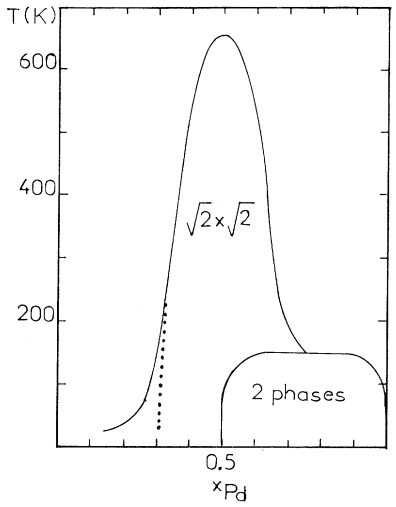

FIG. 4. Phase digram of the CuPd surface alloy on a Cu (001) substrate as calculated with concentration-dependent pairwise interactions. Dotted line: phase diagram calculated with only V_1 for 75% of Cu atoms.

ed, however, with a smooth variation of the dominating positive nearest-neighbor interchange interaction as a function of the composition. Another interesting feature is that for the $Cu_{75}Pd_{25}$ alloy, the second- and third-nearest-neighbor pair interactions are orders of magnitude smaller than the first-nearest-neighbor pair interaction. Thus, on the Cu-rich side of the phase diagram, the influence of the pair interactions beyond the first-nearest neighbors are negligible in comparison with the behavior observed at 25 or 50% of Cu atoms. The phase diagram obtained with the concentration-dependent pair interactions is displayed in Fig. 4 in which for the technical reasons the MC simulations were stopped at 25 K. A comparison with Fig. 3 indicates an appreciable change. The Cu-rich part is modified due to the strong stability of the $c(2\times2)$, since V_1 becomes more positive in this region with the other pair interactions being negligible. Consequently, a new behavior at low temperature is observed: the first-order transition is missed if all the pair interactions beyond the first-nearest neighbors are strictly taken equal to zero. (This case corresponds to the part of the phase diagram shown as dotted line.) The asymmetrical shape of the phase diagram seems to be able to interpret the conclusions obtained from the LEED patterns,[20] namely that the $c(2\times2)$ structure is found at a Pd coverage in the region of 0.5 and 0.8 ML. According to the calculated phase diagram, it is impossible to find a $c(2\times2)$ structure for a Pd coverage smaller than 0.3 at a reasonable finite temperature. On the other hand, the $c(2\times2)$ phase displays a stability range that extends to a monolayer coverage of Pd. In this case, however, the $c(2\times2)$ structure is in thermodynamical equilibrium with a pure Pd phase. It should be noted that according to the surface-energy contribution, Pd on a Cu(001) surface is not stable and some Pd may be dissolved in the Cu below the $c(2\times2)$ surface. This effect has not been taken into account in the present calculations but can also be treated[19] theoretically.

ACKNOWLEDGMENTS

The financial support for this work was provided by the Grant Agency of the Academy of Sciences of the Czech Republic (Project No. 110 437), the Grant Agency of the Czech Republic (No. 202/93/0688), and the Austrian Science Foundation (P 10231). Monte Carlo simulations have been performed using a CPU-time allocation at the computer center of the CNRS (IDRIS).

[1]F. Ducastelle, *Order and Phase Stability* (North-Holland, Amsterdam, 1991).

[2]J. W. Connolly and A. R. Williams, Phys. Rev. B **27**, 5169 (1983).

[3]F. Ducastelle, in *Alloy Phase Stability,* Vol. 163 of *NATO Advanced Study Institute, Series B: Physics,* edited by A. Gonis and G. M. Stocks (Kluwer, London, 1989), p. 293.

[4]K. Terakura, T. Oguchi, T. Mohri, and K. Watanabe, Phys. Rev. B **35**, 2169 (1987).

[5]A. Zunger, in *Statics and Dynamics of Alloy Phase Transformations,* Vol. 319 of *NATO Advanced Study Institute Series B: Physics,* edited by P. E. A. Turchi and A. Gonis (Plenum, New York, 1994), p. 361, and references therein.

[6]J. M. Sanchez, J. P. Stark, and V. L. Moruzzi, Phys. Rev. B **44**, 5411 (1991).

[7]M. Asta, D. de Fontaine, M. van Schilfgaarde, M. Sluiter, M. Methfessel, Phys. Rev. B **46**, 5055 (1992).

[8]M. Sluiter, D. de Fontaine, X. Q. Guo, R. Podloucky, and A. J.

Freeman, Phys. Rev. B **42**, 10 460 (1990).
[9]A. Pasturel, C. Colinet, A. T. Paxton, and M. van Schilfgaarde, J. Phys. Condens. Matter **3**, 7895 (1991).
[10]A. Qteish and R. Resta, Phys. Rev. B **37**, 1308 (1988).
[11]P. A. Sterne and L. T. Wille, Physica C **162-164**, 223 (1989).
[12]G. Ceder, M. Asta, W. C. Carter, M. Kraitchman, D. de Fontaine, M. E. Mann, and M. Sluiter, Phys. Rev. B **41**, 8698 (1990).
[13]L. Udvardi, L. Szunyogh, A. Pasturel, and P. Weinberger, Philos. Mag. B **69**, 683 (1994).
[14]B. Legrand, G. Treglia, and F. Ducastelle, Phys. Rev. B **41**, 4422 (1990); G. Treglia, B. Legrand, and F. Ducastelle, Europhys. Lett. **7**, 575 (1988).
[15]H. Dreyssé, L. T. Wille, and D. de Fontaine, Solid State Commun. **78**, 355 (1991).
[16]V. Drchal, J. Kudrnovský, L. Udvardi, P. Weinberger, and A. Pasturel, Phys. Rev. B **45**, 14 328 (1992).
[17]O. K. Andersen and O. Jepsen, Phys. Rev. Lett. **53**, 2571 (1984).
[18]J. Kudrnovský, S. K. Bose, and V. Drchal, Phys. Rev. Lett. **69**, 308 (1992).
[19]A. Pasturel, V. Drchal, J. Kudrnovský, and P. Weinberger, Phys. Rev. B **48**, 2704 (1993).
[20]S. C. Wu, S. H. Lu, Z. Q. Wang, C. K. C. Lok, J. Quinn, Y. S. Li, D. Tian, F. Jona, and P. M. Marcus, Phys. Rev. B **38**, 5363 (1988).
[21]J. Kudrnovský, P. Weinberger, and V. Drchal, Phys. Rev. B **44**, 6410 (1991).
[22]J. Kudrnovský, I. Turek, V. Drchal, P. Weinberger, N. E. Christensen, and S. K. Bose, Phys. Rev. B **46**, 4222 (1992); J. Kudrnovský, I. Turek, V. Drchal, P. Weinberger, S. K. Bose, and A. Pasturel, *ibid.* **47**, 16 525 (1993).
[23]B. Wenzien, J. Kudrnovský, V. Drchal, and M. Šob, J. Phys. Condens. Matter **1**, 9893 (1989).
[24]J. Kudrnovský, I. Turek, A. Pasturel, R. Tetot, V. Drchal, and P. Weinberger, Phys. Rev. B **50**, 9603 (1994).
[25]V. Drchal, J. Kudrnovský, and P. Weinberger, Phys. Rev. B **50**, 7903 (1994).
[26]J. B. Staunton, D. D. Johnson, B. L. Gyorffy, and C. Walden, Philos. Mag. B **61**, 773 (1990).
[27]R. Kikuchi, Phys. Rev. **81**, 988 (1951).
[28]K. Binder, *The Monte Carlo Method in Condensed Matter Physics* (Springer-Verlag, Berlin, 1991).
[29]P. W. Palmberg and T. N. Rhodin, J. Chem. Phys. **49**, 134 (1968).
[30]Z. Q. Wang, Y. S. Li, C. K. C. Lok, J. Quinn, F. Jona, and P. M. Marcus, Solid State Commun. **62**, 181 (1987).
[31]G. W. Graham, Surf. Sci. **171**, L432 (1986).
[32]G. W. Graham, P. J. Schmitz, and P. A. Thiel, Phys. Rev. B **41**, 3353 (1990).
[33]S. H. Lu, Z. Q. Wang, S. C. Wu, C. K. C. Lok, J. Quinn, Y. S. Li, D. Tian, F. Jona, and P. M. Marcus, Phys. Rev. B **37**, 4296 (1988).
[34]T. D. Pope, G. W. Anderson, K. Griffiths, P. R. Norton, and G. W. Graham, Phys. Rev. **44**, 11 518 (1991).
[35]W. Schweika, K. Binder, and D. P. Landua, Phys. Rev. Lett. **65**, 3321 (1990).